

Photon recycling in Fabry–Perot micro-cavities based on Si_3N_4 waveguides

F. Riboli^{a,*}, A. Recati^b, N. Daldosso^a, L. Pavesi^a, G. Pucker^c,
A. Lui^c, S. Cabrini^d, E. Di Fabrizio^d

^aDepartment of Physics, University of Trento, Via Sommarive 14, Povo, I-38050 Trento, Italy

^bCRS BEC-INFN, Via Sommarive 14, Povo, I-38050 Trento, Italy

^cMicrosystems Division, ITC-IRST, Via Sommarive 18, Trento 38050, Italy

^dINFN-TASC Laboratory, LILIT Beamline, S.S.14 Km 163.5, 34012 Trieste, Italy

Received 29 September 2005; received in revised form 6 December 2005; accepted 6 December 2005
Available online 4 January 2006

Abstract

We present a numerical analysis and preliminary experimental results on one-dimensional Fabry–Perot micro-cavities in Si_3N_4 waveguides. The Fabry–Perot micro-cavities are formed by two distributed Bragg reflectors separated by a straight portion of a waveguide. The Bragg reflectors are composed of a few air slits produced within the Si_3N_4 waveguides. In order to increase the quality factor of the micro-cavities, we have minimized, with a multiparametric optimization tool, the insertion loss of the reflectors by varying the length of their first pairs (those facing the cavity). To explain the simulation results, the coupling of the fundamental waveguide mode with radiative modes in the Fabry–Perot micro-cavities is needed. This effect is described as a recycling of radiative modes in the waveguide. To support the modelling, preliminary experimental results of micro-cavities in Si_3N_4 waveguides realized with the focused ion beam technique are reported.

© 2006 Elsevier B.V. All rights reserved.

PACS: 42.70.Qs; 42.82.Bq; 42.82.Cr; 78.20.Bh

Keywords: Waveguide photonic crystals; Fabry–Perot micro-cavities; Engineered mirrors; Recycling of leaky modes

1. Introduction

Silicon-based photonics is the key technology for manipulating, controlling, and detecting light at sub-micrometer length scales [1]. Owing to the index contrast between silicon-based materials and air, which span from 1 for Si_3N_4 up to 2.5 for Si, these systems are ideal to study devices associated with photonic band-gap materials. Among these, electromagnetic resonant cavities, able to trap light, can be considered as building

blocks of future photonic circuits [2]. In these systems, the confinement of the photons within a finite volume is ensured by a periodic refractive index modulation of the surrounding medium. The best choice is a three-dimensional refractive index modulation that provides a full confinement of photons in the cavities. Nevertheless, there are many difficulties in fabricating three-dimensional periodic structures operating at infrared wavelengths. As a consequence, it seems to be favorable to explore new devices with two- or one-dimensional (1D) refractive index modulation for which the fabrication technology is well established; light confinement in the other dimensions can be realized by total internal reflection within optical

* Corresponding author. Tel.: +39 0461 882070;
fax: +39 0461 881696.

E-mail address: riboli@science.unitn.it (F. Riboli).

waveguides. Photonic crystals based on such an approach exhibit a quasi-photonic band-gap, due to the lack of three-dimensional confinement. An implementation of 1D photonic crystals are photonic crystal slab waveguides, where a high-index core layer is sandwiched between lower index claddings. The 1D refractive index modulation is achieved by producing air trenches across the ridge waveguide. A 1D photonic crystal with a defect is also described as a Fabry–Perot micro-cavity. This is formed by two first order Bragg mirrors separated by a spacer. The Bragg mirrors are constituted by a sequence of $\lambda/2$ thick periods, where each period contains an air slit and a waveguide segment. A photon mode propagating in the ridge waveguide excites many cavity radiative modes when it is transmitted through the cavity. This fact degrades the quality factor (Q -factor) of the cavity. Indeed, the key point for high Q -factor cavities relies on a fine tuning of the lengths of air slits and waveguide pieces (hereafter called coupling pairs) facing the cavity spacer [3–5] to reduce the excitation of radiative cavity modes and decrease the impedance mismatch between waveguide and cavity modes. Nevertheless, the physics beyond these effects is not completely understood, and it is still under debate [6].

The aim of this work is to characterize and optimize the performance of a 1D Fabry–Perot (FP) micro-cavity centered at 1550 nm and formed in a Si_3N_4 ridge waveguide. We start by optimizing the insertion losses of a distribute Bragg reflector (DBR) via engineering the first pairs facing the waveguide spacer, as proposed in [5]. Then, we use the optimized mirrors to build an FP micro-cavity and we study the quality factor (Q -factor) of the optimized system as a function of the resonance order. In the second part of the work, we show that the classical FP model of the Q -factor is unable to explain the numerical results. These can be understood by considering the recycling of radiative modes in the waveguide [7]. In the last part of this work, we report preliminary experimental data on an FP micro-cavity. The FP micro-cavity has been realized with focused ion beam (FIB) processing, starting from a single mode Si_3N_4 ridge waveguide and removing waveguide slices to define the photonic structure. Our modelling is able to explain the experimental data. The full theoretical characterization and realization of other devices are currently in progress to further validate the numerical predictions.

The numerics have been performed by modelling the ridge waveguide with a planar one. Using an effective index approximation [8], we have checked that the effect of the lateral confinement is not relevant for the obtained results.

2. Engineered mirror for high Q -factor device

Classical FP micro-cavities on waveguides are formed by a straight waveguide surrounded by two identical DBR. The main limitation of these systems is the modal mismatch between the fundamental cavity mode (waveguide mode) and the fundamental Bloch mode of the DBR. This mismatch causes strong coupling of the resonant guided mode with radiative modes of the DBR, decreasing the performance of the micro-cavity [9]. Thus an optimization of the coupling between waveguide and DBR is needed. The first step is to consider the problem related to the reflection of a transverse electric (TE) mode impinging from a monomodal waveguide onto a DRB (see Fig. 1(a) for a sketch).

As a material system we choose Si_3N_4 waveguides since we are investigating them as a substitute for more expensive silicon on an insulator waveguide [10]. A monomode Si_3N_4 waveguide formed by a multilayer core of Si_3N_4 and SiO_2 , and a top-bottom cladding of SiO_2 will be considered hereafter (see Section 4 for more details). The waveguide is interfaced to a first order Bragg mirror with a period of 490 nm composed by air slits (width 100 nm) etched 1 μm down through

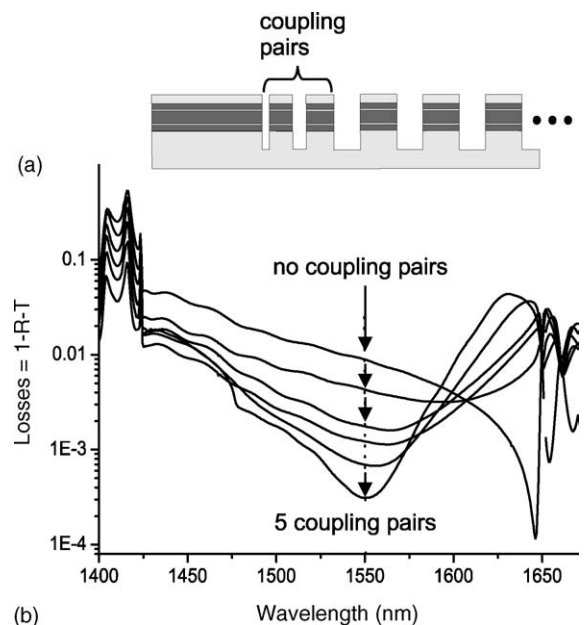


Fig. 1. (a) Cross-view of the simulated system composed by the input waveguide and the mirror where the coupling pairs are emphasized. (b) Insertion losses of six optimized mirrors, $L = 1 - R - T$, as a function of the wavelength. The mirrors differ by the number of coupling pairs which face the input waveguide. The arrows are a guide for the eye to follow the results as the number of coupling pairs increases.

the bottom cladding. With these parameters the DBR supports a single guided TE polarized Bloch mode – a mode below the light-line. The characterization of the waveguide–mirror interface is made by exciting the fundamental waveguide mode and calculating the reflection R (transmission T) coefficient of this mode through the waveguide–DBR system. The insertion loss spectra, defined as $L = 1 - R - T$, are calculated from 1.4 to 1.7 μm , which includes the DBR stop band region. All the simulations have been made with a commercial software [11] based on an eigenmode expansion (EME) method [12]. The minimization of the insertion losses is made by means of a multiparametric optimization tool.

Optimization of the insertion losses is completed by inserting coupling pairs at the interface between the waveguide and the DBR. The physical lengths of each air slit and waveguide segment in the coupling pairs are the free parameters of the multiparametric optimization. The numerical results of the optimization are shown in Fig. 1(b) where the insertion loss spectra of six optimizations are reported as a function of wavelength. The six curves correspond to different numbers of coupling pairs, varying from zero (no coupling pairs) to five. While increasing the number of coupling segments, a well-defined minimum appears at 1.55 μm ; the insertion losses are decreased by two orders of magnitude from 10^{-2} for the bare mirror to 3×10^{-4} for the five pairs engineered mirror. Table 1 reports the parameters of the coupling pairs for the five mirrors. For each engineered mirror we report the pair lengths, Λ , and the filling fractions, f.f. (the ratio between the length of air slit and the pair).

The engineered mirrors have been then used to form optimized micro-cavities (Fig. 2). Fig. 3 reports their calculated Q -factor as a function of the resonance order, m , when no (circles), one (triangles) and two (squares) coupling pairs are used. The micro-cavity intrinsic Q -factor was calculated from the asymptotic value of the full width at half maximum $\Delta\lambda$ of the

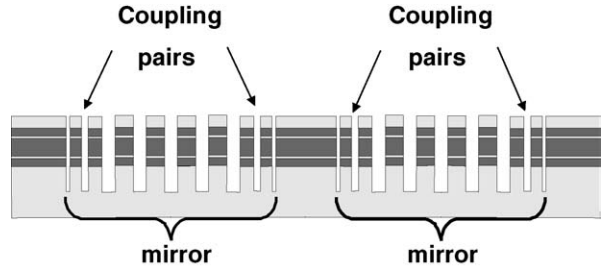


Fig. 2. Schematic lateral view of a micro-cavity with optimized mirrors. The system is composed of an input–output waveguide, two engineered mirrors, and a spacer. Each engineered mirror has coupling pairs facing the waveguide and the spacer.

resonant peak as the number of DBR periods increase, while the number of coupling pairs is kept constant; knowing the micro-cavity resonance wavelength $\lambda_0 = 1.55 \mu\text{m}$, $Q_{\text{int}} = \lambda_0 / \Delta\lambda$. The resonance order is defined as in Eq. (3). For the smallest defect length the minimum value of m is about 4, due to the large penetration depth of the mode defect in the mirror (see also the discussion after Eq. (3)).

As expected, it is seen that the Q -factor increases as the number of coupling pairs increases, since the insertion losses of the mirrors L decrease as shown in Fig. 1. For instance, at $m \approx 9$ we have $Q \approx 3 \times 10^3$, 1.1×10^4 , 5.1×10^4 for no, one, and two coupling pairs, respectively. On the other hand, it is clearly seen that such an increase is not very regular as m changes. Such a behavior is discussed in the next section.

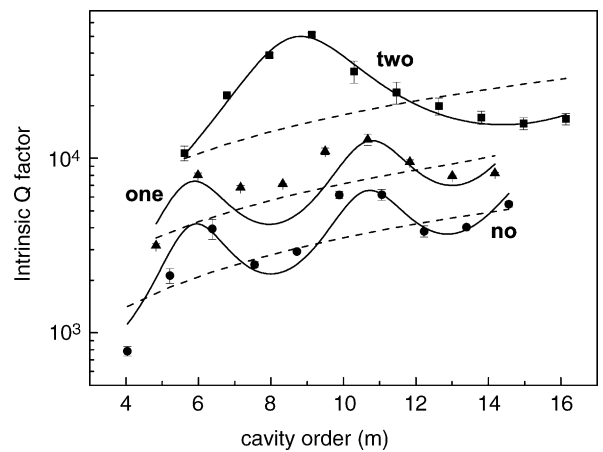


Fig. 3. Q -factor of micro-cavities with no (circle), one (triangle) and two (square) coupling pairs in the engineered mirrors as a function of the resonance order. Points refer to numerical results, the dashed lines are the classical FP prediction and the continuous lines are the predictions from the FP model with effective reflectivity coefficient for the fundamental mode.

Table 1
Coupling pair lengths Λ and filling fractions f.f. for the five engineered mirror (Λ (nm)/f.f.)

| Number of coupling pairs | | | | |
|--------------------------|-------------|-------------|-------------|-------------|
| 1 | 2 | 3 | 4 | 5 |
| 423.4/0.236 | 453.3/0.195 | 446.9/0.14 | 468.2/0.158 | 458.4/0.144 |
| | 424.7/0.247 | 447.8/0.194 | 429.7/0.133 | 447.6/0.147 |
| | | 454.2/0.283 | 474.2/0.238 | 456.7/0.196 |
| | | | 446.2/0.294 | 464.9/0.242 |
| | | | | 450/0.293 |

For the periodic mirror $\Lambda = 490 \text{ nm}$ and f.f.=0.204.

3. Interpretation of the simulation results

Let us consider an FP cavity with mirrors characterized by complex reflectivity and transmissivity coefficients, $r = |r| e^{i\varphi_m}$ and $t = |t| e^{i\varphi_m}$, respectively; the spacer between the two mirrors is characterized by a physical length, L , and by an effective refractive index, n_{eff} . The expression of the cavity transmission is given by the Airy formula

$$t_{\text{FP}} = \frac{t^2 e^{i\Phi}}{1 - r^2 e^{i\Phi}}, \quad (1)$$

where the phase accumulated by the electromagnetic wave after the half round-trip in the cavity is

$$\Phi = \frac{2\pi}{\lambda} n_{\text{eff}} L + \varphi_m. \quad (2)$$

Under the assumption that $1 - |r|^2 \ll 1$, the quality factor of the micro-cavity can be expressed as

$$Q = \frac{|r|}{1 - |r|^2} \left[\frac{2\pi}{\lambda} n_g L - \lambda \frac{\partial \varphi_m}{\partial \lambda} \right]_{\lambda=\lambda_0} \equiv \frac{|r|}{1 - |r|^2} m\pi, \quad (3)$$

where λ_0 is the resonant wavelength, $n_g = n_{\text{eff}} - \lambda(\partial n_{\text{eff}}/\partial \lambda)$ is the group index of cavity mode. In Eq. (3), we have also identified the resonance order m with the term in square brackets divided by π . The second term in brackets is proportional to the penetration depth in the mirror.

The dashed lines in Fig. 3 are the Q -factors predicted by Eq. (3) for the micro-cavities with no, one, and two coupling pairs in the DBRs, respectively. In our case, n_{eff} of Eq. (2) is the effective refractive index of the waveguide defining the micro-cavity. Only the order of magnitude is obtained by this model, while the oscillations in the Q -factors found in the simulations are not reproduced. It is thus needed to go beyond this simple model and use more accurate models, which predict a nonlinear dependence of the Q -factor on the mode order. In particular, the theory in Ref. [7] considers that not only the fundamental Bloch mode of the micro-cavity is excited by the fundamental waveguide mode but also radiative cavity modes. It is worth mentioning these radiative cavity modes can be coupled back into the transmitted waveguide mode, a phenomenon which can be described as a recycling of photons in the waveguide by the micro-cavity. Hence, not only the fundamental cavity mode contributes to determine the Q -factor of the micro-cavity but also the

radiative ones. The constructive (destructive) interference among the cavity modes, which eventually increases (decreases) the Q -factor, depends on the cavity parameters (physical length, modal reflectivity). Following Ref. [7], the radiative cavity modes are described by a single leaky cavity mode with two complex parameters, a complex coefficient for the coupling of the cavity leaky mode with the fundamental mode $r' e^{i\theta}$ and a complex effective index of the leaky mode itself $n' + in''$. Thus, the whole process can be described by an effective reflectivity coefficient for the waveguide fundamental mode, which depends on the resonance order $r_{\text{eff}}(m; r', \theta, n', n'')$. The Q -factor is then given by an FP-like expression with the dressed reflectivity coefficient $r_{\text{eff}}(m)$ [7],

$$Q = \frac{|r_{\text{eff}}(m)|}{1 - |r_{\text{eff}}(m)|^2} m\pi. \quad (4)$$

The continuous lines in Fig. 3 show the predictions of this model when the two complex parameters $r' e^{i\theta}$ and $n' + in''$ are chosen such that Q fits the simulated data. The agreement in this case is pretty good, suggesting that the recycling of the leaky mode could play an important role in determining the performance of such micro-cavities. Even if the fit parameters have no strict physical meaning, we have checked to determine if they take values compatible with leaky mode representation: the effective index of leaky mode is lower than that of the cladding, the real part of the coupling coefficient satisfies the energy conservation.

4. Preliminary experimental results

To validate the positive role of the coupling pairs to increase the micro-cavity Q -factors, we present some preliminary experimental results for a system realized by the focused ion beam (FIB) technique starting from an Si_3N_4 single mode waveguide. As a side-result, we show that the FIB technique can be effectively used to form 1D photonic crystals with good optical quality without the need to go through the lithography and etching steps used in other processing.

Slab multilayer waveguides were fabricated by a low-pressure chemical vapor deposition (LPCVD) on a 2.5 μm thick SiO_2 . It consists of the following sequence of Si_3N_4 and SiO_2 : 100 nm Si_3N_4 , 50 nm SiO_2 , 200 nm Si_3N_4 , 50 nm SiO_2 and 100 nm Si_3N_4 [13]. This results in a total core layer thickness of about 500 nm. The core was capped with a 500 nm thick cladding SiO_2 layer. Lithography and etching

define ridge waveguide geometries, whose nominal widths ranged from 1 to 10 μm . The 1D-PhC structures were defined on the ridge by using a 30 KeV Ga+ FIB [14,15]. In our experiment, we used the LEO-ZEISS 1540XB CrossBeam[®], comprising a high resolution FIB column to mill directly in combination with a high precision scanning electron microscope (SEM) for precise positioning and inspection of the fabricated nanostructures in real time. Using an ion current of about 100 pA and controlling the FIB by a pattern generator (RAITH ELPHY), the pattern is directly written on the sample surface; using a total ion dose of 400 mA/cm², a depth of about 1.3 μm for each structure was obtained. Fig. 4(a) shows a top view scanning electron microscopy (SEM) image of a Fabry–Perot sample with one coupling pair.

The optical properties of integrated optical micro-cavities have been characterized by coupling in light from a tunable laser (1300–1630 nm, 2 mW) through a single mode polarization maintaining tapered fiber, mounted on a nano-positioning system. Two linear polarizers and a half-wave plate are used to control the polarization of the input signal. The collection system

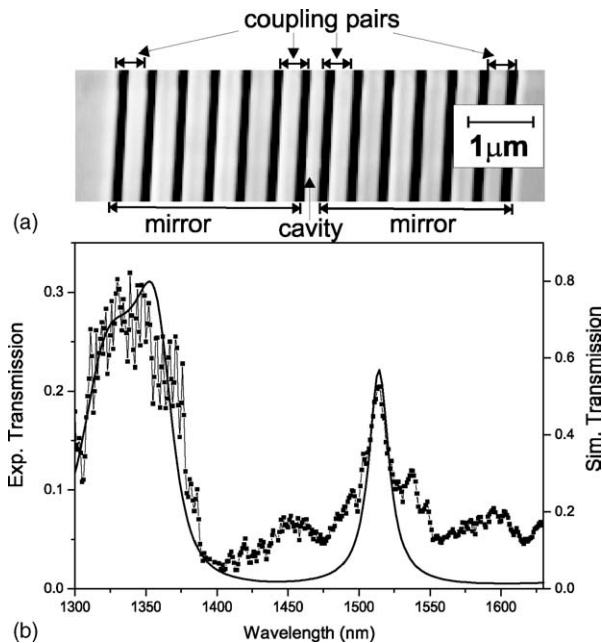


Fig. 4. (a) Top view SEM image of the cavity with one segment engineered mirror. (b) Relative transmittance of the transverse electric (TE) polarized light of the cavity shown in (a). The points show the experimental data and the continuous line represents the numerical simulation. The nominal/simulation parameters are $\Lambda = 435$ nm/450 nm and f.f.=0.23/0.244 for the coupling pair, $\Lambda = 490$ nm/510 nm and f.f.=0.204/0.215 for the periodic mirror, and 190 nm/172 nm for the cavity defect.

was provided by a near field microscope objective matched to a variable zoom mounted on a high-performance InGaAs infrared camera controlled by the LBA-500 Spiricon beam analyzer software. A prism beam splitter allows a directly transmitted signal to a calibrated photodiode (Ge detector) to perform intensity measurements. Normalization of the transmission intensity is completed with respect to a nearby reference waveguide without the 1D photonic crystals.

Fig. 4(b) shows the relative transmittance of transverse electric (TE) polarized light for the engineered FP micro-cavity of Fig. 4(a). The measured spectrum shows a well-defined band-edge at 1380 nm and the resonant peak at 1515 nm. The first FP oscillation (corresponding to the interference of Bloch modes of the 1D system) can be observed between 1300 and 1380 nm. The measured full width at half maximum (FWHM) of the resonance peak is 15 nm, which corresponds to a quality factor $Q = 105$.

The spectrum is compared to the numerical calculations (line in Fig. 4(b)) and a reasonable good agreement is found for the spectral position of the FP stop band, the resonance position and width, while the baseline in the photonic band-gap region is not reproduced due to diffraction losses and light leakages not taken into account in the calculations. The parameters (length of air slits and waveguide segments) used to reproduce the spectrum are slightly different from the nominal one by about 5–10%. The Q -factor calculated with a classical FP model is larger by a factor of two than the measured one. This can be a good indication that anti-recycling of the leaky modes into the fundamental mode occurs in this sample. Clearly, other effects can affect the measured low Q values, which are mostly related to the quality of the 1D photonic structures however, photon recycling effects are surely playing a role and only a more systematic study of these engineered structures could weigh the relative importance of the photon recycling effect. Such a study is under way.

5. Conclusions

In this work we have presented preliminary testing of the effect of photon recycling, which occurs in a 1D photonic crystal when guided and radiative modes interfere. Simulations and first measurements show this effect should not be underestimated in optimizing the Q -factors of micro-cavities, based on 1D photonic crystals.

Acknowledgements

We acknowledge the financial support by MIUR through FIRB (RBNE01P4JF and RBNE012N3X) and COFIN (2004023725) projects and by PAT through PROFILL project.

References

- [1] L. Pavesi, D. Lockwood (Eds.), *Silicon Photonics: Topics in Applied Physics*, vol. 94, Springer-Verlag, Berlin, 2004.
- [2] K.J. Vahala, *Nature* 424 (2003) 839–846.
- [3] B.S. Song, S. Noda, T. Asano, Y. Akahane, *Nat. Mater.* 4 (2005) 207.
- [4] G. Steven, S. Johnson, A. Fan, J.D. Mekiş, Joannopoulos, *Appl. Phys. Lett.* 78 (2001) 3388.
- [5] P. Lalanne, J.P. Hugonin, *IEEE J. Quant. Electr.* 39 (2003) 1430.
- [6] C. Sauvan, P. Lalanne, J.P. Hugonin, *Nature* 429 (2004) 6988.
- [7] Ph. Lalanne, M. Mias, J.P. Hugonin, *Opt. Exp.* 12 (2004) 458.
- [8] K. Sakoda, *Fundamentals of Optical Waveguides*, Academic Press, San Diego, CA, USA, 2000.
- [9] F. Riboli, N. Daldosso, G. Pucker, A. Lui, L. Pavesi, *IEEE J. Quant. Electron.* 41 (2005) 1197.
- [10] N. Daldosso, M. Melchiorri, F. Riboli, M. Girardini, G. Pucker, M. Crivellari, P. Bellutti, A. Lui, L. Pavesi, *IEEE J. Lightwave Technol.* 22 (2004) 1734.
- [11] Photon Design Software: FimmWave and FimmProp version 4.2, 2004.
- [12] A.S. Sudbo, *IEEE Phot. Technol. Lett.* 5 (1993) 342.
- [13] M. Melchiorri, N. Daldosso, F. Sbrana, L. Pavesi, G. Pucker, C. Kompochois, P. Bellutti, A. Lui, *Appl. Phys. Lett.* 86 (2005) 121111.
- [14] K.A. Valiev, *The Physics of Sub-micron Lithography*, Plenum Press, 1992.
- [15] S. Cabrini, A. Carpentiero, R. Kumar, L. Businaro, P. Candeloro, M. Prasciolu, A. Gosparini, L.C. Andreani, M. De Vittorio, T. Stomeo, E. Di Fabrizio, *Microelectron. Eng.* 11 (2005) 78–79.